DMD Fast Forward. Published on December 29, 2020 as DOI: 10.1124/dmd.120.000276
This article has not been copyedited and formatted. The final version may differ from this version.

Evaluation of the Utility of PXB Chimeric Mice for Predicting Human Liver Partitioning of Hepatic Organic Anion-Transporting Peptide Substrates

Bo Feng, Rachel Pemberton, Wojciech Dworakowski[1], Zhengqi Ye, Craig Zetterberg, Guanyu Wang, Yoshio Morikawa and Sanjeev Kumar

Drug Metabolism and Pharmacokinetics, Vertex Pharmaceuticals, Boston, Massachusetts (B.F., R.P., W.D., Z.Y., C.Z., G.W., S.K.); PhoenixBio USA Corporation, New York City, New York (Y.M.)

[1]Current affiliation: Syros Pharmaceuticals, Cambridge, Massachusetts

DMD Fast Forward. Published on December 29, 2020 as DOI: 10.1124/dmd.120.000276
This article has not been copyedited and formatted. The final version may differ from this version.

Running Title: Human liver partitioning of OATP substrates

Corresponding Author: Bo Feng, 50 Northern Ave, Vertex Pharmaceuticals, Boston, Massachusetts 02210, E-mail: Bo_Feng@vrtx.com, Phone: (617) 961-0150

Number of text pages: 28

Number of Tables: 5

Number of Figures: 6

Number of References: 60

Abstract word count: 249

Introduction word count: 1046

Discussion word count: 2755

ABBREVIATIONS: OATP, organic anion-transporting polypeptide; SCID, severely compromised immune-deficient mice; PXB, urokinase plasminogen activator/severe combined immunodeficiency (uPA/SCID) mice repopulated with over 90% human hepatocytes; AUC, area under the plasma concentration-time curve; DHP, dehydropravastatin; Fu,plasma, fraction unbound of plasma; Fu,liver, fraction unbound of liver; K_{puu}, unbound partition coefficient; LC-MS/MS, liquid chromatography-tandem mass spectrometry; PET, positron emission tomography; PK, pharmacokinetics; DDIs, drug-drug interactions; PD, pharmacodynamics.

DMD Fast Forward. Published on December 29, 2020 as DOI: 10.1124/dmd.120.000276
This article has not been copyedited and formatted. The final version may differ from this version.

Abstract

The ability to predict human liver-to-plasma unbound partition coefficient (K_{puu}) is important to estimate unbound liver concentration for drugs that are substrates of hepatic organic anion transporting peptide (OATP) transporters with asymmetric distribution into the liver relative to plasma. Herein, we explored the utility of PXB chimeric mice with humanized liver that are highly repopulated with human hepatocytes to predict human hepatic disposition of OATPs substrates, including rosuvastatin, pravastatin, pitavastatin, valsartan and repaglinide. In vitro total uptake clearance and transporter-mediated active uptake clearance in C57 mouse hepatocytes were greater than PXB chimeric mouse hepatocytes for rosuvastatin, pravastatin, pitavastatin and valsartan. Consistent with in vitro uptake data, enhanced hepatic uptake and resulting total systemic clearance were observed with the above four compounds in control SCID than in PXB chimeric mouse, which suggest that mouse has a stronger transporter-mediated hepatic uptake than human. In vivo liver-to-plasma K_{puu} from PXB chimeric and SCID control mice were also compared, and rosuvastatin and pravastatin K_{puu} in SCID mouse were more than 10-fold higher than that in PXB chimeric mouse, whereas, pitavastatin, valsartan and repaglinide K_{puu} in SCID mouse were comparable with K_{puu} in PXB chimeric mouse. Finally, PXB chimeric mouse liver-to-plasma K_{puu} values were compared with the reported human K_{puu}, and a good correlation was observed as the PXB K_{puu} vales were within 3-fold of human K_{puu}. Our results indicate that PXB mice could be a useful tool to delineate hepatic uptake and enable prediction of human liver-to-plasma K_{puu} of hepatic uptake transporter substrates.

DMD Fast Forward. Published on December 29, 2020 as DOI: 10.1124/dmd.120.000276
This article has not been copyedited and formatted. The final version may differ from this version.

Significance Statement

We evaluated PXB mouse with humanized liver for its ability to predict human liver disposition of five OATP transporter substrates. Both in vitro and in vivo data suggest that mouse liver has a stronger transporter-mediated hepatic uptake than the humanized liver in PXB mouse. More importantly, PXB liver-to-plasma K_{puu} values were compared with the reported human K_{puu}, and a good correlation was observed. PXB mice could be a useful tool to project human liver-to-plasma K_{puu} of hepatic uptake transporter substrates.

DMD Fast Forward. Published on December 29, 2020 as DOI: 10.1124/dmd.120.000276
This article has not been copyedited and formatted. The final version may differ from this version.

Introduction

Assessment of unbound liver drug concentration is critical for understanding the pharmacological activity and developing pharmacokinetic (PK)/pharmacodynamics (PD) relationships for disease targets residing in the liver, predicting metabolic and biliary clearance as well as drug-drug interactions (DDIs) potential, and anticipating the risk of liver adverse events. According to pharmacokinetic principles, it is often assumed that, for permeable compounds that distribute into non-eliminating tissues via passive diffusion, unbound tissue concentration equals unbound plasma concentration at equilibrium. However, this assumption may not hold true in the case of liver which expresses a variety of uptake and efflux drug transporters as well as drug metabolizing enzymes. Based on the extended clearance concept, the unbound partition coefficient (K_{puu}) between the liver and plasma in vivo is governed by a balance of passive diffusion, intrinsic clearance of active hepatic uptake, sinusoidal and biliary efflux, and metabolism (Shitara and Sugiyama, 2006; Watanabe et al., 2010; Yabe et al., 2011). Hence, unbound plasma concentrations cannot always serve as a surrogate for unbound liver concentrations. When drugs are actively taken up into liver through hepatic uptake transporters, such as organic anion-transporting proteins (OATPs) and/or are metabolized in the liver, K_{puu} can be significantly different than unity. During drug discovery efforts focused at disease targets located in the liver, it is of great interest to accurately predict in vivo liver-to-plasma K_{puu} in humans, since it enables direct estimation of the unbound liver concentrations, which are challenging to measure directly in humans, from the easily measurable unbound plasma concentrations. Accurate assessment of human liver-to-plasma K_{puu} thus can help facilitate the design of drugs with targeted distribution to the liver, modeling of DDIs due to

DMD Fast Forward. Published on December 29, 2020 as DOI: 10.1124/dmd.120.000276
This article has not been copyedited and formatted. The final version may differ from this version.

inhibition/induction of liver enzymes and transporters, and development of PK/PD relationships when transporters are involved in the asymmetric hepatic drug distribution process.

The ability to predict in vivo liver-to-plasma K_{puu} from in vitro assays is highly desirable, but a direct extrapolation of in vitro results to in vivo K_{puu} in humans is challenging because transporter protein levels and function in the in vitro systems could be quite different than those in vivo (Bow et al., 2008; Kunze et al., 2014; Morse et al., 2015; Vildhede et al., 2015). Meanwhile, the translational value of traditional preclinical animal models to humans is limited by the substantial species differences in hepatic transporter homology, sequence identity, expression pattern, substrate specificity and affinity (Chu et al., 2013; Grime and Paine, 2013). OATPs are expressed on the sinusoidal membrane of hepatocytes and have been identified as main contributors to the disposition of statins and a number of other drug classes (Ieiri et al., 2009). The impact of OATPs on hepatic clearance of their substrates has been demonstrated via OATP1B1 polymorphisms and DDIs with OATP inhibitors. (Neuvonen et al., 2006; Ieiri et al., 2009; Kalliokoski and Niemi, 2009; Niemi et al., 2011; Yoshida et al., 2012). The significant species differences in amino acid sequences between human OATPs and rodent Oatps make it difficult to translate PK or PD data from preclinical species to humans. In an attempt to overcome these limitations, different humanized animal models have been developed to gain insight into the determinants of liver drug disposition and bridge the gap between preclinical to clinical extrapolation. For example, knockout models lacking murine Oatp1a/1b isoforms and OATP1B1- or OATP1B3- humanized transgenic mice have been developed to estimate the pharmacokinetics of human OATP substrate drugs (van de Steeg et al., 2013; Zimmerman et al., 2013; Higgins et al., 2014; Salphati et al., 2014). However, the presence of three major hepatic OATPs in the human liver with broad overlap in substrate specificity could result in a different

DMD Fast Forward. Published on December 29, 2020 as DOI: 10.1124/dmd.120.000276
This article has not been copyedited and formatted. The final version may differ from this version.

drug disposition profile relative to these transgenic mice that express each OATP individually. Additionally, mouse liver metabolism could be much different from human.

Another well-studied humanized model is the PXB mice, which are chimeric mice with humanized liver that express the urokinase plasminogen activator (uPA+/+) gene on a severely compromised immune-deficient (SCID) background (Tateno et al., 2015). These PXB mice have constitutive expression of a protease in mouse hepatocytes causing hepatic injury and thus permit the selective expansion of fully functional human hepatocytes upon transplantation. The livers of these mice can be highly (up to > 90-95%) repopulated with human hepatocytes, and based on mRNA and protein measurements, the expression levels of drug-metabolizing enzymes and drug transporters in hepatocytes of PXB mice were similar to those in human livers (Tateno et al., 2004; Nishimura et al., 2005; Okumura et al., 2007; Ohtsuki et al., 2014). PXB chimeric mice with humanized liver have been used for human PK prediction (Sanoh et al., 2012; Miyamoto et al., 2017; Naritomi et al., 2019), human-specific metabolite identification (Samuelsson et al., 2012; Bateman et al., 2014), and DDI studies (Katoh et al., 2007; Uchida et al., 2018).

The purpose of our studies was to evaluate the utility of PXB chimeric mouse model to predict liver disposition of OATP substrates in humans. To this end, systemic PK and liver distribution of five OATP substrates, including rosuvastatin, pravastatin, pitavastatin, valsartan, and repaglinide, were studied in PXB vs. SCID mice and compared with the available clinical data on their hepatic disposition. In addition, uptake kinetics of these five OATP substrates were characterized in plated hepatocytes from PXB and C57 mouse to compare with the findings from in vivo studies. These drugs have been reported to interact with the hepatic OATPs in either in vitro systems and/or in clinical studies involving patients with polymorphic variants of OATP1B1 to support the contributing role of active uptake in their liver disposition (Ieiri et al.,

2009; Niemi et al., 2011). Moreover, these drugs have also been associated with clinical DDIs due to inhibition of active transport, either in isolation or in conjunction with a reduction in metabolism (Hirano et al., 2006; Ieiri et al., 2009; Prueksaritanont et al., 2014). Given that the in vivo disposition of many OATP substrates is complex - involving multiple elimination pathways via various drug transporters and metabolizing enzymes - PXB chimeric mice could be a promising model for preclinical to clinical translation of hepatic drug disposition. However, understanding the PK and liver disposition of different OATP substrates in these mice relative to humans is essential before they can be used for mechanistic understanding and translational studies in drug discovery and development.

DMD Fast Forward. Published on December 29, 2020 as DOI: 10.1124/dmd.120.000276
This article has not been copyedited and formatted. The final version may differ from this version.

Materials and Methods:

Materials. Plateable mouse hepatocytes isolated from C57 mice were purchased from BioIVT (Hicksville, NY, USA). PXB hepatocytes were isolated from chimeric PXB mice and freshly plated by PhoenixBio (Hiroshima, Japan). Hepatocyte plating and maintenance media were composed of Williams E medium supplemented with either Primary Hepatocyte Thawing and Plating or Primary Hepatocyte Maintenance Supplements (ThermoFisher Scientific, Waltham, MA, USA). Universal Cryopreservation Recovery Medium (UCRM)was obtained from In Vitro ADMET Laboratories (Columbia, MD, USA). 24-well collagen I – coated plates were purchased from BD Biosciences (Oxford, UK). Bicinchoninic Acid (BCA) protein assay was purchased from Sigma-Aldrich (St. Louis, MO). Test compounds were obtained from Sigma-Aldrich or internal Vertex archive (Boston, MA).

Animal Husbandry. Mice were kept in Techniplast Green Line individually ventilated mouse cages. Autoclaved food and water were available *ad libitum*. Light cycles were on a 12:12 light/dark cycle with the lighting phase starting at 0630 hours. Temperature and relative humidity were maintained between 21°C and 23°C and 30% to 70%, respectively. Animals were acclimatized for at least 72 hr before starting an experimental procedure.

Animals and Treatments. All animal studies were approved by Institution for Animal Care and Use (IACUC) within Association for Assessment and Accreditation of Laboratory Animal Care (AAALAC) accredited vivarium. PXB male mice were obtained from PhoenixBio (Hiroshima, Japan) at ages 16-22 weeks, and SCID male mice were purchased from Charles River Laboratories (Wilmington, MA) model #236 at an age range of 10-12 weeks that were further aged in house to be 12-16 weeks at time of study. Mice were dosed orally with one of the following OATP substrates: rosuvastatin calcium, pravastatin sodium, valsartan, and repaglinide,

DMD Fast Forward. Published on December 29, 2020 as DOI: 10.1124/dmd.120.000276
This article has not been copyedited and formatted. The final version may differ from this version.

and pitavastatin calcium. Initially, each substrate was administered at varying single doses according to table 1 in PXB and SCID mice (n = 3 per substrate) with whole blood samples collected out to 24 hr in order to assess dose vs. exposure relationship. Subsequently, these data were used to select doses for our primary goal of measuring liver-to-plasma K_{puu} at clinically relevant systemic exposure. During the K_{puu} studies, substrates were dosed in PXB and SCID mice (4-5 mice per compound per strain) via oral administration using varying regimens according to table 2. Terminal plasma and liver were collected at T_{max} (formally determined from single dose PK studies) for each substrate according to table 2. The vehicles used to formulate the OATP substrates were the same for single dose PK and K_{puu} studies.

Tissue and Blood/Plasma Sampling. Whole blood samples (10 µl blood: 40 µl water) were collected via the tail vein at 30 min, 1 hr, 2 hr, 4 hr, 7 hr, and 24 hr for pharmacokinetic analyses. Blood was mixed with 40 µl of deionized water immediately after collection and then placed on dry ice. Whole blood samples were stored at -80°C until analysis.

For K_{puu} evaluation, plasma was collected via the vena cava at T_{max}, followed by cardiac perfusion with heparinized saline (50 µL of 1000 USP units/mL heparin per mL saline)Prior to perfusion, animals were aestheticized with ketamine (40 mg/mL) and xylazine (2 mg/mL) dosed IP 0.1 mL per 10 g body weight. Liver was resected, weighed, and placed on dry ice. Liver samples were homogenized in phosphate buffer (typically 3-fold dilution) for concentration determination, and the samples were further diluted as needed for the liver homogenate binding assay.

Plasma Protein Binding and liver binding Assays. Rapid Equilibrium Dialysis (RED) plates and inserts (MWCO: 8K) were purchased from Thermo Fisher Scientific (Waltham, MA). Dialysis phosphate buffer (100 mM sodium phosphate in 150 mM NaCl, pH 7.4) was prepared in

DMD Fast Forward. Published on December 29, 2020 as DOI: 10.1124/dmd.120.000276
This article has not been copyedited and formatted. The final version may differ from this version.

house. The internal standard (IS) was a proprietary compound synthesized in house. Plasma dilution method was used as needed for the plasma protein binding assay. Aliquots (200 µL) of plasma, diluted plasma or liver homogenate samples were loaded into the donor chamber of the RED device for dialysis against 350 µL of the phosphate buffer. The loaded RED device was sealed with an adhesive membrane and agitated at ~450 rpm for 18 hr (plasma) or 6 hr (liver homogenate) in the 37°C incubator with 85% humidity. The assay was performed in triplicate. Time zero samples were prepared by adding an aliquot of the plasma, diluted plasma or liver homogenate sample prior to dialysis to an equal volume of buffer and extracted with the IS solution in acetonitrile. After incubation, an aliquot of the sample was taken from the donor side of the RED device and added to an equal volume of buffer and extracted with the IS solution in acetonitrile. An aliquot of the dialysate sample was taken from the receiver side of the RED device and added to an equal volume of blank matrix (plasma, diluted plasma or liver homogenate) and extracted with the IS solution. Samples were vortexed, centrifuged at 2950 g for 20 min, and the supernatants were transferred to 96-well plates for LC-MS/MS analysis.

Fraction Unbound Data Analysis.

Fraction unbound: $Fu = (C_{free}/C_{total})$

C_{free} = Peak area ratio of the compound in the dialysate (receiver side) after incubation

C_{total} = Peak area ratio of the compound in plasma or liver homogenate (donor side) after incubation

Formula for calculating fraction unbound Fu (corrected) from Fu (uncorrected) (fraction unbound in diluted matrix):

Fu_(corrected)) = (1/D)/([1/ Fu_(uncorrected)) - 1] + 1/D) where D = dilution factor.

DMD Fast Forward. Published on December 29, 2020 as DOI: 10.1124/dmd.120.000276
This article has not been copyedited and formatted. The final version may differ from this version.

Quantification of Rosuvastatin, Pravastatin, Pitavastatin, Valsartan, Repaglinide in Whole Blood, Plasma and Liver Samples. The whole blood samples were lysed with 4 parts of water and extracted with the IS solution in acetonitrile at an aqueous-to-organic ratio of 1:10. The plasma and liver homogenate samples were extracted with the IS solution in acetonitrile at an aqueous-to-organic ratio of 1:10. Samples were vortexed and centrifuged at 2254 g for 20 min. The extract was injected onto LC-MS/MS for concentration determination.

LC-MS/MS Analysis. The LC-MS/MS analysis was performed on an API 5500 QTrap or 6500+ triple quadrupole mass spectrometer (AB Sciex, Framingham, MA) equipped with Agilent 1200 or 1290 series binary pumps from Agilent Technologies (Santa Clara, CA) and a CTC Analytics PAL autosampler (CTC Analytics AG, Zwingen, Switzerland). Mobile phase A was 10 mM ammonium acetate (pH 4) and mobile phase B was methanol/acetonitrile (1:1, v/v). The liquid chromatographic analysis was performed on a Unisol C18 column (2.1 × 30 mm, 5 μm) from Agela Technologies (Wilmington, DE). The analyte was eluted using a gradient method with an initial mobile phase composition of 100% A at a flow rate of 800 μL/min. The mobile phase B increased from 0% to 70% in 0.3 min and was hold at 70% for 0.7 min before being ramped up to 99% in 0.2 min. The mobile phase was kept at 99%B for 1 min at an increased flow rate of 1800 μL/min. It was then brought back to the initial condition in 0.3 min.

Pitavastatin, valsartan, repaglinide, rosuvastatin, and the IS were monitored in positive electrospray ionization (ESI) mode using multiple reaction monitoring (MRM) transitions of m/z 422 → 290, m/z 436 → 235, m/z 453 → 230, m/z 482 → 258, and m/z 406 → 346, respectively. Pravastatin and the IS were monitored in negative ESI mode using MRM transitions of m/z 423 → 321 and m/z 404 → 102, respectively.

DMD Fast Forward. Published on December 29, 2020 as DOI: 10.1124/dmd.120.000276
This article has not been copyedited and formatted. The final version may differ from this version.

For plasma protein binding and tissue binding assays, quantitation of the compounds was based on peak area ratio of the compound versus the IS. For the PK studies, quantitation of the compounds was based on calibration curves prepared in blank matrix (plasma, liver homogenate, or a mixture of whole blood/water at 1:4). A fit-for-purpose method qualification was performed for all analytes. The lower limit of quantitation (LLOQ) in whole blood analysis was 5.0 ng/mL for rosuvastatin. The LLOQ in plasma was 1.0 ng/mL for pravastatin, repaglinide, rosuvastatin and valsartan; and 2.5 ng/mL for pitavastatin. The LLOQ in liver sample was 1.0 ng/g for pravastatin, repaglinide and valsartan; 2.5 ng/g for pitavastatin; and 10 ng/g for rosuvastatin. The accuracy of the methods met the acceptance criteria of ±20% of nominal concentrations. The precision (CV) met the acceptance criteria of ≤ 20%. The summary of QC sample data is presented in supplemental table.

Pharmacokinetic Analysis. Descriptive statistics of whole blood concentrations and pharmacokinetic parameter estimates were calculated using the Watson LIMS Version 7.4 software. AUC_{last} value was calculated using the linear trapezoidal rule. Pharmacokinetic parameters for all substrates were obtained by non-compartmental analysis. The slope of the elimination phase (λ_z) was estimated by linear regression. Maximum whole blood concentration (C_{max}) and time to C_{max} (t_{max}) were obtained directly from the observed values. Log-transformed plasma concentrations were plotted against Log-transformed Kp_{uu} values.

In Vitro Hepatocytes Uptake Studies. Cryopreserved hepatocytes were rapidly thawed in a 37°C bath and poured into prewarmed UCRM tubes. Mouse hepatocytes were centrifuged at 100g, then resuspended in plating media. Cell number and viability were determined using trypan blue exclusion. All hepatocyte suspensions seeded for uptake experiments contained >80% viable cells. Cells were diluted to a density of 0.4×10^6 cells/mL, and 0.5 mL was added to

DMD Fast Forward. Published on December 29, 2020 as DOI: 10.1124/dmd.120.000276
This article has not been copyedited and formatted. The final version may differ from this version.

each well of a 24-well collagen I - coated plate. Plates were incubated for 4 hr in a humidified chamber at 37°C/5% CO_2 to allow cell attachment. Plating media was replaced with maintenance media and incubated overnight prior to initiating experiments. Hepatocyte uptake of OATP substrates was measured at a single concentration of 0.1 µM, with exceptions for pravastatin (5 µM) and valsartan (1 µM) due to analytical and permeability characteristics. Total and passive clearance was determined from the initial rate of uptake at 37°C in the absence and presence of the OATPs inhibitor, 1 mM rifamycin SV. Cell monolayers were rinsed twice and preincubated with 250 µl HBSS containing 1 mM rifamycin SV or DMSO solvent for at least 15 min. Incubations were initiated by adding 250 µl prewarmed volumes of 2X substrate drug ± 1 mM rifamycin SV to duplicate wells. Substrate was added at 30 s intervals for a total incubation time of two minutes, at which time aliquots were collected for analysis. The incubation was terminated by removal of remaining substrate solutions and washing the cell monolayers three times on ice with cold HBSS. Cells were frozen at -20°C, and subsequently lysed for 10 min in acetonitrile solution containing an analytical internal standard (tolbutamide). Lysates were mixed with an equal volume of water and transferred into tubes for centrifugation at 8385 g Supernatants were submitted for LC-MS/MS analysis to determine intracellular concentration of intracellular fraction, in addition to the unbound concentration of incubation solutions. Representative samples in each assay were treated as above but lysed in RIPA buffer to measure total protein by the BCA assay.

LC-MS/MS Analysis of Hepatocytes Uptake. Samples were analyzed using an Agilent 1100 series high-performance liquid chromatography (HPLC) system (Agilent, Santa Clara, CA) paired with a SCIEX triple quadrupole 6500+ mass spectrometer (SCIEX, Framingham, MA). Aliquots were injected onto a Unisol C18 column (5 µm, 2.1 × 30 mm; Agela Technologies,

DMD Fast Forward. Published on December 29, 2020 as DOI: 10.1124/dmd.120.000276
This article has not been copyedited and formatted. The final version may differ from this version.

Newark, DE) using a CTC Analytics PAL (LEAP) autosampler (CTC Analytics AG, Zwingen, Switzerland). The analytes and internal standard were eluted using a gradient method with a flow rate from 0.8 to 1.8 mL/min. Mobile phase A was 10 mM ammonium acetate in water (pH 4.0) and mobile phase B was acetonitrile/methanol (50/50, v/v). The peak area ratio of analyte/internal standard was quantified by standard regression, including only standards with response within 30% of nominal concentration. A fit-for-purpose method qualification was performed as well for all the analytes. The LLOQ was 50 pM. The same analysis acceptance criteria as described earlier were applied for each analytical run. The summary of QC sample data is presented in supplemental table.

Determination of Hepatocyte Kinetic Uptake Parameters. Total uptake (CLuptake) and passive clearance (CLpassive) values were measured by the rate of hepatocyte uptake in the absence and presence of an OATP inhibitor, 1 mM rifamycin SV, respectively. The initial rate of uptake was determined over 2 min including four time points, 0.5, 1, 1.5 and 2 min, as the slope of the linear regression of the intracellular concentration vs. time plot. CLuptake and CLpassive were calculated by dividing slope by the measured average unbound concentration of the incubation solutions, and normalizing to protein content. Active uptake clearance (CLactive) was calculated by subtracting CLpassive from CLuptake. The differences of *in vitro* hepatocyte uptake clearance between C57 and PXB mice were evaluated by unpaired t-test with p-value of 0.05.

DMD Fast Forward. Published on December 29, 2020 as DOI: 10.1124/dmd.120.000276
This article has not been copyedited and formatted. The final version may differ from this version.

Results

In Vitro Uptake of five OATP substrates in C57 mouse and PXB chimeric mouse hepatocytes

Five OATP substrates, including rosuvastatin, pitavastatin, pravastatin, valsartan and repaglinide, were investigated in the plated C57 mouse and PXB chimeric mouse hepatocytes. Unbound uptake clearance and passive diffusion were measured from initial rates at 0.5, 1.0, 1.5 and 2 min in the absence and presence of the OATP inhibitor, 1 mM rifamycin SV, respectively. The unbound uptake clearance (CLuptake) and transporter-mediated unbound active uptake clearance (CLactive) are presented in Fig 1. For rosuvastatin, pravastatin and valsartan, CLuptake and CLactive in C57 mouse hepatocytes were substantially higher (close to 10-fold) than that in PXB mouse hepatocytes. In the case of pitavastatin, CLuptake and CLactive in C57 mouse hepatocytes were moderately higher (2-4-fold) than PXB mouse hepatocytes. Whereas, CLuptake and CLactive in C57 mouse and PXB chimeric mouse hepatocytes were comparable for repaglinide. Additionally, active uptake contributed to more than 90% of total uptake of rosuvastatin, pravastatin, pitavastatin and valsartan in mouse hepatocytes, while, the relative contribution of active transport to total uptake of repaglinide was much smaller (~65%) in mouse hepatocytes (Fig. 1). Interestingly, the relative contribution of active transport to the total uptake was more profound in C57 mouse than PXB chimeric mouse hepatocytes. Particularly for pravastatin and pitavastatin, active uptake contributed to more than 90% of total uptake in C57 mouse hepatocytes, but only ~60% of total uptake in PXB hepatocytes. It is worth pointing out that we were unable to acquire hepatocytes from control SCID mouse and tested the five OATP substrate in hepatocytes from C57 mouse instead. Hence, it is possible that the hepatocytes from C57 mouse function somewhat differently from SCID mouse.

DMD Fast Forward. Published on December 29, 2020 as DOI: 10.1124/dmd.120.000276
This article has not been copyedited and formatted. The final version may differ from this version.

PK of rosuvastatin, pitavastatin, pravastatin, valsartan and repaglinide in PXB and SCID mice

Systemic PK of the five OATP substrates, including rosuvastatin, pitavastatin, pravastatin, repaglinide and valsartan, were assessed in PXB and SCID mice. Following single oral administration of each compound, whole blood samples were collected for full PK profile up to 24 hr in PXB and the control SCID mice to assess dose-exposure relationship. The results from dose-proportionality PK studies (Table 1) were used to determine the doses necessary to reach the reported clinical Cmax for liver-to-plasma K_{puu} studies. The reported clinical Cmax, measured human Fu,plasma and calculated free Cmax, as well as the doses chosen for K_{puu} studies of five compounds are summarized in table 2. Unbound fractions of five compounds in plasma and liver were determined by rapid equilibrium dialysis (Table 3) to calculate unbound plasma and unbound liver concentrations (Table 4) for liver-to-plasma K_{puu} estimations. Statistical significance of liver-to-plasma K_{puu} between PXB and SCID mouse was determined by unpaired student t-test with a p-value of 0.05. Rosuvastatin ($p<0.01$) showed the most significant difference.

In vivo K_{puu} measurement of Rosuvastatin.

The reported rosuvastatin clinical Cmax is 44 ng/mL (Luvai et al., 2012), which equates to ~7.5 ng/mL unbound rosuvastatin in plasma with a human fu,plasma of 17.1% (internal data). Based on dose-proportionality studies, single doses of 15 and 30 mg/kg for SCID mice and 1.5 and 3 mg/kg for PXB mice were selected for liver-to-plasma rosuvastatin K_{puu} measurements (Table 2). It is worth mentioning that we have evaluated and compared the K_{puu} values from multiple dose studies where rosuvastatin was dosed BID for three days to reach steady state or after a

DMD Fast Forward. Published on December 29, 2020 as DOI: 10.1124/dmd.120.000276
This article has not been copyedited and formatted. The final version may differ from this version.

single dose with samples at Tmax, and the K_{puu} values from the two methods were comparable. Thus, plasma and liver concentrations of rosuvastatin were measured at Tmax for each single dose. The plasma and liver binding of rosuvastatin in PXB and SCID mice were determined by rapid equilibrium dialysis (Table 3) to calculate unbound plasma and unbound liver concentrations (Table 4). Fig. 2 shows rosuvastatin liver-to-plasma K_{puu} values in both PXB and SCID mice at unbound plasma concentration matching the free Cmax in human, and the data clearly indicated that rosuvastatin K_{puu} was dramatically increased in SCID mice relative to PXB mice. The average rosuvastatin liver-to-plasma K_{puu} in PXB mice was ~23, which was more than 10-fold lower than the average rosuvastatin K_{puu} of ~268 in SCID mice (Fig. 2). The data in Fig. 2 also demonstrated that although the dose in SCID mice was 10-fold higher than the dose in PXB mice, the unbound plasma concentrations in PXB and SCID mice were similar suggesting more profound hepatic uptake in SCID mice compared with PXB mice. This is consistent with the observation that hepatic uptake of rosuvastatin (and resulting systemic clearance) in SCID mouse was much greater than in PXB mouse in the dose-proportionality study of rosuvastatin (Table 1).

In vivo K_{puu} measurement of pravastatin

Based on the reported clinical Cmax (25 ng/mL) of pravastatin (Hatanaka, 2000), 0.6 and 3 mg/kg for PXB mice and multiple dose levels (1.8, 3, 10, 20 and 40 mg/kg) for SCID mice were selected for pravastatin liver-to-plasma K_{puu} evaluation, as well as understanding the relationship between the unbound plasma concentrations in PXB and SCID mice and K_{puu} (Table 2). Unbound fractions of pravastatin in plasma and liver were determined (Table 3) to calculate unbound plasma and unbound liver concentrations (Table 4). Fig. 3 depicts pravastatin liver-to-

DMD Fast Forward. Published on December 29, 2020 as DOI: 10.1124/dmd.120.000276
This article has not been copyedited and formatted. The final version may differ from this version.

plasma K_{puu} in PXB and SCID mice, and the data revealed that greater systemic exposures in SCID mice correlated with lower K_{puu} values, which is likely due to the saturation of hepatic uptake transporters. At approximate human pravastatin unbound Cmax (~13 ng/mL), the liver-to-plasma K_{puu} in PXB mice was ~4.4, whereas, the K_{puu} in SCID mice was ~121, which is in agreement of the previous reports (Higgins et al., 2014; Salphati et al., 2014) and remarkably larger than K_{puu} in PXB mice. Additionally, more than 20-fold higher dose of pravastatin was needed in SCID mice as compared to PXB mice to reach the unbound clinical Cmax, indicating that the hepatic uptake (and as a result, systemic clearance) of pravastatin in SCID mice was considerably higher than that in PXB mice, which is also consistent with the observation in pravastatin dose-proportionality study (Table 1).

In vivo K_{puu} measurement of pitavastatin

Based on the reported clinical Cmax of pitavastatin (38 ng/mL) (Luo et al., 2015), 0.1/0.2 mg/kg and 0.2/0.5 mg/kg of pitavastatin were dosed in PXB and SCID mice, respectively, for liver-to-plasma K_{puu} measurements (Table 2). Pitavastatin unbound fractions in plasma and liver were measured (Table 3) to calculate unbound plasma and unbound liver concentrations of pitavastatin (Table 4), as well as liver-to-plasma K_{puu} (Fig. 4). In contrast to rosuvastatin and pravastatin, pitavastatin liver-to-plasma K_{puu} of ~16 in PXB mice at the unbound pitavastatin plasma concentration matching the approximate clinical unbound Cmax, was similar to the K_{puu} of ~18 in the control SCID mice, which is consistent with the previously reported liver-to-plasma K_p of ~20 in FVB mice (Salphati et al., 2014). As expected, hepatic uptake of pitavastatin in PXB mice was weaker than in SCID mice but to a much less extent than rosuvastatin and pravastatin. These

DMD Fast Forward. Published on December 29, 2020 as DOI: 10.1124/dmd.120.000276
This article has not been copyedited and formatted. The final version may differ from this version.

data suggest that the hepatic uptake (and as a result, systemic clearance) of pitavastatin in SCID mice was slightly higher than that in PXB mice.

In vivo K_{puu} measurement of valsartan

Based on the reported clinical Cmax (3250 ng/mL) of valsartan (Siddiqui et al., 2011), 8 mg/kg valsartan was dosed in SCID mice, and 5 and 8 mg/kg valsartan were dosed in PXB mice to generate valsartan liver-to-plasma K_{puu} (Table 2). Interestingly, valsartan liver-to-plasma K_{puu} in PXB mice was about 2-fold higher than K_{puu} in SCID mice, with an average valsartan K_{puu} of ~82 in PXB mice and ~40 in SCID mice at the approximate human unbound Cmax of valsartan, as shown in Fig. 5. Aligning with the single dose PK studies (Table 1), the valsartan total Cmax values in PXB mice were strikingly higher than those in SCID mice in K_{puu} studies. However, since SCID mouse plasma fu of valsartan is ~10-fold higher than PXB mouse plasma fu (Table 3), the free plasma concentrations of valsartan in SCID mice were only ~2-fold lower than those in PXB mice at the same dose, suggesting that the hepatic uptake (and as a result, unbound systemic clearance) of valsartan in SCID mice was only modestly higher (~2-fold) than that in PXB mice.

In vivo K_{puu} measurement of repaglinide

Similar to the previous studies, based on the reported clinical Cmax (65 ng/mL) of repaglinide (Hatorp, 2002), 1.5 and 1 mg/kg and 0.8 mg/kg of repaglinide were dosed into SCID and PXB mice, respectively, for liver-to-plasma K_{puu} studies. Repaglinide liver and plasma protein binding in PXB and SCID mice were determined (Table 3) to calculate unbound plasma and unbound liver concentrations (Table 4), as well as K_{puu} (Fig 6). Repaglinide liver-to-plasma K_{puu}

DMD Fast Forward. Published on December 29, 2020 as DOI: 10.1124/dmd.120.000276
This article has not been copyedited and formatted. The final version may differ from this version.

values were indistinguishable between PXB and SCID mice, with values slightly higher than 1 in both cases. Additionally, the systemic clearance of repaglinide in SCID and PXB mice was also similar in the K_{puu} study, which is consistent with the observation in dose proportionality study of repaglinide. These data imply that hepatic uptake of repaglinide (and resulting systemic clearance) in SCID and PXB mice are similar.

DMD Fast Forward. Published on December 29, 2020 as DOI: 10.1124/dmd.120.000276
This article has not been copyedited and formatted. The final version may differ from this version.

Discussion:

The utility of animal models in understanding drug disposition and its extrapolation to human is challenging due to differences in enzyme and transporter substrate specificity as well as expression levels across species (Hagenbuch and Meier, 2003; Chu et al., 2013; Grime and Paine, 2013). On the other hand, certain clinical pharmacology or mechanistic studies cannot be conducted in humans for ethical and practical reasons. Therefore, humanized animal models could be very valuable to bridge the gap between preclinical and clinical to understand the determinants of human drug disposition. PXB chimeric mice with humanized liver have been successfully used for metabolite profiling, PK prediction, and DDI studies. However, to the best of our knowledge, no studies using PXB mice to predict human liver disposition of hepatic uptake transporter substrates have been reported. Hence, a comprehensive understanding of the PK and liver disposition of different hepatic OATP substrates, , in these mice is needed before they can be used for translational prediction in drug discovery and development. Given that the in vivo disposition of many OATP substrates is complex, involving multiple elimination pathways via various drug transporters and metabolizing enzymes, we have studied hepatic uptake of five different OATP transporter substrates, including rosuvastatin, pravastatin, pitavastatin, valsartan and repaglinide, in PXB chimeric and the control SCID mice. Liver-to-plasma K_{puu} were measured in both PXB and SCID mice and compared with the published human K_{puu} data from the clinical imaging studies, PK/PD, or in vitro studies. The goal of these studies was to assess PXB mice as a potential tool for studying the role of hepatic uptake transporters in drug disposition in translational research.

The hypothesis was that if the liver of PXB chimeric mouse truly functions like a human liver in terms of both hepatic drug uptake, metabolism and biliary clearance, then the liver

DMD Fast Forward. Published on December 29, 2020 as DOI: 10.1124/dmd.120.000276
This article has not been copyedited and formatted. The final version may differ from this version.

uptake and liver-to-plasma K_{puu} of OATP substrates in PXB mice will be comparable to humans, and different from that in mice. It was reported previously that the active uptake clearance in rat hepatocytes on average was 7.1-fold higher than in human hepatocytes based on a comparison of uptake clearance of seven OATP substrates in rat and human hepatocytes (Ménochet et al., 2012b; Ménochet et al., 2012a). Additionally, human OATP-transgenic mice had a weaker uptake efficiency for statins than control mice (Higgins et al., 2014; Salphati et al., 2014), which could be explained by differences in transporter expression and/or specificity between the two mouse strains. In line with this observation, mouse Oatp expression levels in liver and hepatocytes were reported to be much greater than that in human liver and hepatocytes (Wang et al., 2015). Given that the sequence homology of Oatps between mice and rats is quite high (Meier-Abt et al., 2005), it is expected that there are minimal species differences between rat and mouse Oatps.

First the uptake of the five well characterized OATP substrates, including rosuvastatin, pitavastatin, pravastatin, valsartan and repaglinide, in hepatocytes from C57 mouse and PXB chimeric mouse were characterized (Fig 1). In the case of rosuvastatin, pravastatin and valsartan, the overall and transporter-mediated active uptake clearances in mouse hepatocytes were markedly higher than in PXB chimeric mouse hepatocytes. For pitavastatin, the uptake in mouse hepatocytes was moderately higher than PXB hepatocytes, while repaglinide had a similar uptake in mouse and PXB mouse hepatocytes. As described above, it has been reported previously that rat hepatocytes exhibit greater uptake activities for OATP substrates, and the intrinsic active uptake of rosuvastatin, pravastatin and valsartan in rat hepatocytes was much greater than that in human hepatocytes (Ménochet et al., 2012a; Grime and Paine, 2013); in contrast, repaglinide and pitavastatin active uptake clearance values were within 3-fold of each

other in the two species. Thus, the uptake differences between C57 mouse and PXB mouse hepatocytes observed in our studies are aligned with the reported uptake differences between rat and human hepatocytes. These data substantiate that PXB mouse hepatocytes function more like human hepatocytes. Although in general the expression levels of Oatps are higher in rodents than humans, the substrate affinity towards human transporters could be greater than rodent hepatocytes for drugs such as pitavastatin (Ménochet et al., 2012b). Consequently, the species difference in hepatocyte uptake of pitavastatin is less pronounced than rosuvastatin, pravastatin and valsartan. Despite the species difference in hepatic uptake clearance being compound dependent, in general higher hepatic uptake is observed in rodents than humans. It is not surprising that repaglinide displayed similar uptake in mouse and PXB chimeric mouse hepatocytes, because the transporter contribution to hepatic uptake of highly permeable repaglinide is much less than the other four compounds.

PK studies of the five OATP substrates demonstrated that the total blood exposures to rosuvastatin, pravastatin, and valsartan in PXB chimeric mice were ~10-fold or more higher than that in control SCID mice at the same dose, and the blood exposure to pitavastatin in PXB mice was ~8-fold higher than that in control SCID mice (Table 1). In contrast to these four OATP substrates, the blood exposure to repaglinide in PXB mice was indistinguishable from that in SCID mice at the same dose (Table 1). Considering the plasma binding of rosuvastatin and pravastatin is similar in PXB and SCID mouse, whereas the plasma binding in PXB mouse is higher than SCID mouse for valsartan (~10-fold) and pitavastatin (~3-fold) (Table 3), the unbound plasma concentrations in SCID mice were much lower than PXB mice for rosuvastatin and pravastatin, and slightly lower (~2-fold) for pitavastatin and valsartan. These data suggest that the hepatic uptake of these four compounds in SCID mice is greater than that in PXB mice,

DMD Fast Forward. Published on December 29, 2020 as DOI: 10.1124/dmd.120.000276
This article has not been copyedited and formatted. The final version may differ from this version.

whereas the hepatic uptake of repaglinide in SCID and PXB mice is comparable. These PK data are reasonably in line with in vitro hepatocytes uptake data (Fig 1), which also demonstrated equal uptake of repaglinide in PXB and C57 mouse hepatocytes, but greater uptake of the other four compounds in mouse hepatocytes than PXB mouse hepatocytes. Quantitatively, the uptake difference of valsartan in mouse and PXB hepatocytes in vitro (~10-fold) was considerably higher than the uptake difference in SCID and PXB mouse in vivo (~2-fold), and the reason for this discrepancy remains to be understood. On the other hand, because of a higher passive permeability, the contribution of active uptake to the total hepatic uptake of repaglinide is much less than the aforementioned four OATP substrates, which has been confirmed in DDI studies with OATP inhibitors as well as by the effect of OATP1B1 polymorphisms on repaglinide pharmacokinetics (Kalliokoski et al., 2008; Yoshikado et al., 2017). As a result, the impact of species difference in OATPs/Oatps on hepatic uptake and pharmacokinetics of repaglinide is likely to be smaller. Consistent with the similar hepatic uptake of repaglinide in SCID and PXB mice, the blood exposures to repaglinide in PXB chimeric and SCID mice were comparable.

Since liver-to-plasma K_{puu} can be concentration-dependent, it is important to measure K_{puu} at the plasma concentrations that approximate the unbound Cmax in the clinic. Using data from dose-ranging PK studies, the doses of each compound were selected for K_{puu} study to ensure that the unbound plasma concentrations in PXB mouse were close to the human unbound Cmax. The unbound systemic clearance of rosuvastatin in SCID mouse was considerably greater than in PXB mouse, and rosuvastatin liver-to-plasma K_{puu} in SCID mice was observed to be remarkably higher (>10-fold) than that in PXB mice (Fig. 2). Consistent with our observation, Uchida et al. also reported that the total systemic clearance of rosuvastatin was substantially higher in SCID mice than in PXB mice after intravenous administration, and its blood

DMD Fast Forward. Published on December 29, 2020 as DOI: 10.1124/dmd.120.000276
This article has not been copyedited and formatted. The final version may differ from this version.

concentrations were ~5-fold lower in SCID than in PXB mice (Uchida et al., 2018). Thus, rosuvastatin liver-to-blood K_p was markedly higher (close to 10-fold) in SCID mice than in PXB mice, which indicates a higher uptake in SCID mice than in PXB mice. Moreover, Iusuf et al. (Iusuf et al., 2013) reported that normal mice had lower systemic concentrations of rosuvastatin compared with human OATP transgenic mice, mainly due to a higher liver distribution. Similar to rosuvastatin, pravastatin liver-to-plasma K_{puu} (Fig. 3) in PXB mice was dramatically lower than that in SCID mice. Whereas, pitavastatin (Fig. 4) and repaglinide K_{puu} (Fig. 6) in PXB and SCID mice were similar. Interestingly, valsartan liver-to-plasma K_{puu} (Fig. 5) in PXB mice were ~2-fold of K_{puu} in SCID mice.

According to the extended clearance concept, liver-to-plasma K_{puu} is governed by multiple clearance pathways, including the intrinsic clearance of passive diffusion, active hepatic uptake, sinusoidal efflux, biliary excretion, as well as metabolism. Differences in the metabolism of these OATP substrates in mice and humans can potentially obscure the in vivo impact of the OATP transporters on drug disposition in these two mouse models. Rosuvastatin and pravastatin are hydrophilic with a lower passive permeability than other statins, and their systemic clearance is mostly mediated by hepatic uptake and biliary clearance as well as renal clearance of the unchanged drug, with negligible metabolism in mice and humans (Martin et al., 2003; Kitamura et al., 2008; Iusuf et al., 2013). Furthermore, hepatic uptake of rosuvastatin and pravastatin via OATPs significantly influences their PK rather than biliary efflux via other transporters, because the uptake process is the rate-determining step in their disposition (Shitara and Sugiyama, 2006; Elsby et al., 2012; Shitara et al., 2013). Accordingly, rosuvastatin and pravastatin liver-to-plasma K_{puu} is mainly determined by active hepatic uptake. Thus, K_{puu} in PXB mice is expected to be much smaller than that in SCID mice because of species difference in OATP/Oatp mediated

DMD Fast Forward. Published on December 29, 2020 as DOI: 10.1124/dmd.120.000276
This article has not been copyedited and formatted. The final version may differ from this version.

hepatic uptake as discussed previously. Additionally, the contribution of active uptake to total uptake of pravastatin in PXB hepatocytes was much smaller (~60%) compared with C57 mouse hepatocytes (>95%) (Fig. 1). Consistent with this, the liver-to-plasma K_{puu} of pravastatin in PXB mouse was much lower than that in SCID mice and only modestly greater than unity.

Compared with rosuvastatin and pravastatin, pitavastatin has a higher passive permeability. The unbound plasma concentrations of pitavastatin in PXB mice were slightly higher than SCID mice at the same dose in liver-to-plasma K_{puu} studies, suggesting that the unbound hepatic uptake of pitavastatin in SCID mice is marginally higher than PXB. These observations are consistent with the fact that pitavastatin AUC increases upon co-administration with rifampin (an OATP/oatp inhibitor) were similar in both humans (Prueksaritanont et al., 2014) and mice (internal data), suggesting that hepatic uptake of pitavastatin in human and mouse are similar. Additionally, the major clearance pathway for pitavastatin is Bcrp-mediated biliary clearance, and mouse liver Bcrp expression level is substantial higher (3-8-fold) than human (Chu et al., 2013). Both of these factors could contribute to a similar liver-to-plasma K_{puu} for pitavastatin in SCID and PXB mice.

Although the unbound hepatic uptake and systemic clearance of valsartan in SCID mice were moderately higher than PXB mice (~2-fold), valsartan liver-to-plasma K_{puu} in SCID was ~2-fold lower than PXB mice (Fig 5). It has been reported that MRP2-mediated biliary clearance plays a prominent role in valsartan liver disposition, and the unbound valsartan biliary clearance in rats was ~35-fold higher than that in humans (Grime and Paine, 2013), which is consistent with the report that the amount of Mrp2 in rat liver was approximately 10-fold greater than that in human (Li et al., 2009; Wang et al., 2015; Fallon et al., 2016). It is possible that a much greater biliary clearance of valsartan in SCID mouse partially masked the difference in liver-to-

DMD Fast Forward. Published on December 29, 2020 as DOI: 10.1124/dmd.120.000276
This article has not been copyedited and formatted. The final version may differ from this version.

plasma K_{puu} values of valsartan between PXB and SCID mice. In the case of repaglinide, both hepatic active uptake and metabolism are important determinants of its hepatic clearance (Patilea-Vrana and Unadkat, 2016). As discussed previously, the contribution of active uptake to the total hepatic uptake of repaglinide was much smaller than other compounds. As such, repaglinide liver-to-plasma K_{puu} in PXB and SCID mice are anticipated to be comparable and close to unity. Additionally, although the uptake clearance of valsartan was much lower than repaglinide, since the contributions of active uptake to total uptake were substantially higher for valsartan than repaglinide in PXB and mouse hepatocytes (Fig. 1), it is not surprising that valsartan liver-to-plasma K_{puu} were much higher than repaglinide in both SCID and PXB mice.

The ultimate objective of these studies was to compare liver-to-plasma K_{puu} in PXB mice with human K_{puu} to validate whether PXB mice would be an acceptable translational model to predict human liver disposition of hepatic uptake transporter substrates. It should be noted that K_{puu} values are concentration-dependent, and higher plasma concentrations can saturate hepatic uptake transporters, leading to lower K_{puu}. Pravastatin K_{puu} data have clearly demonstrated that K_{puu} decreased with higher plasma concentrations of pravastatin (Fig. 3). Therefore, the dosing duration and regimen in PXB mice were appropriately selected to ensure that K_{puu} values were determined at clinically relevant in vivo exposure. A comparison of the measured liver-to-plasma K_{puu} from PXB mice, SCID mice and human K_{puu} from positron emission tomography (PET), PK/PD modeling, and in vitro human hepatocytes is shown in Table 5. The measured K_{puu} from PXB mice are in good agreement with the reported human liver K_{puu} (within 2-fold), except for pitavastatin. High-quality in vivo human K_{puu} data are relatively very scarce since liver biopsy is invasive and PET imaging has some limitations (e.g., interference from metabolites, non-specific binding to tissues). Thus, very few in vivo human K_{puu} values are available for comparison with

DMD Fast Forward. Published on December 29, 2020 as DOI: 10.1124/dmd.120.000276
This article has not been copyedited and formatted. The final version may differ from this version.

PXB mice. Human liver PET data has been reported for [^{11}C] rosuvastatin (Billington et al., 2019) and its liver-to-plasma K_p was estimated to be ~38 using the terminal-phase (after 15 min) of rosuvastatin liver and plasma data. Then K_p was corrected with our in-house-measured rosuvastatin human Fu,p of 17.1% and PXB mouse Fu,liver of 19.1% to estimate liver-to-plasma K_{puu} of ~43 in human, which is within 2-fold of rosuvastatin K_{puu} of ~23 observed in PXB mouse study. Besides rosuvastatin, human liver PET data has also been reported for [^{11}C]dehydropravastatin (DHP) (Kaneko et al., 2018), an analog of pravastatin. With the similar transporter interactions between DHP and pravastatin, the K_{puu} value of DHP could be used as a surrogate for the K_{puu} of pravastatin. The K_{puu} was estimated to be ~7 using terminal-phase (after 15 min) of DHP data with pravastatin human Fu,p of 52.0% and human Fu,liver of 49.0% (Internal data), which is within 2-fold of pravastatin liver-to-plasma K_{puu} of ~4.4 measured in PXB mice. Moreover, human K_{puu} values of rosuvastatin and pravastatin have been calculated using PK/PD modeling. These estimates carry some uncertainty because these are indirectly derived from a number of in vitro and in vivo parameters. Nevertheless, rosuvastatin human K_{puu} of ~10 was estimated from PK/PD (Riccardi et al., 2017), which is ~2-fold of rosuvastatin K_{puu} of ~23 in PXB mice. In addition, pravastatin liver-to-plasma K_{puu} of ~5.3 was estimated based on PK/PD (Riccardi et al., 2017), which is also close to the pravastatin K_{puu} of ~4.4 measured in PXB mice. Due to lack of human PET and PK/PD modeling data, human liver-to-plasma K_{puu} of pitavastatin, valsartan and repaglinide were generated from in vitro human hepatocytes (Table 5) (De Bruyn et al., 2018). The data indicate that the K_{puu} values of valsartan and repaglinide from PXB mice are similar to those generated in human hepatocytes. However, pitavastatin PXB mouse K_{puu} of ~14 is almost 10-fold higher than the K_{puu} of 1.7 generated using in vitro hepatocytes. Interestingly, another group reported pitavastatin liver-to-plasma K_{puu} values from

2.10-14.58 using different methods in human hepatocytes (Riede et al., 2017). The reason for the discrepancy is not yet clear, and further studies are warranted to understand this disconnect. It is possible that in vitro hepatocytes data could misrepresent in vivo human K_{puu} due to the different hepatic uptake transporter expressions and functions between in vitro and in vivo settings. Overall, given the uncertainty of the human K_{puu} values from PET, PK/PD modeling and human hepatocytes, the K_{puu} for the five OATP substrates from PXB mice appear to suggest a reasonable translational accuracy for the model. To further evaluate the utility of PXB mice for predicting human liver partitioning of hepatic OATP substrates, high quality human liver PET or biopsy data are greatly desired.

In summary, our data suggest that PXB chimeric mice with humanized liver offer promise for gaining an understanding of human hepatic uptake and the anticipated human liver-to-plasma K_{puu} in drug discovery and development, which can help develop the confidence for preclinical to clinical translation of liver drug disposition. This model can be a potentially useful tool for quantitative ADME characterization and mechanistic studies, particularly for drugs where multiple enzymes/transporters play a role in their disposition.

Acknowledgements

The authors thank Chimeric Mouse with Humanized Liver (CMHL) Consortium for the support of the study.

Authorship contributions

Participated in research design: Feng, Pemberton, Dworakowski & Kumar

Conducted experiments: Pemberton, Zetterberg, Ye

Contributed new reagents or analytic tools: Zetterberg, Ye, Morikawa

Performed data analysis: Feng, Pemberton, Zetterberg, Ye, Wang

Wrote or contributed to the writing of the manuscript: Feng, Pemberton, Ye, Zetterberg, Kumar

References:

Bateman TJ, Reddy VGB, Kakuni M, Morikawa Y, and Kumar S (2014) Application of Chimeric Mice with Humanized Liver for Study of Human-Specific Drug Metabolism. *Drug Metabolism and Disposition* **42:**1055-1065.

Billington S, Shoner S, Lee S, Clark-Snustad K, Pennington M, Lewis D, Muzi M, Rene S, Lee J, Nguyen TB, Kumar V, Ishida K, Chen L, Chu X, Lai Y, Salphati L, Hop C, Xiao G, Liao M, and Unadkat JD (2019) Positron Emission Tomography Imaging of [(11) C]Rosuvastatin Hepatic Concentrations and Hepatobiliary Transport in Humans in the Absence and Presence of Cyclosporin A. *Clin Pharmacol Ther* **106:**1056-1066.

Bow DA, Perry JL, Miller DS, Pritchard JB, and Brouwer KL (2008) Localization of P-gp (Abcb1) and Mrp2 (Abcc2) in freshly isolated rat hepatocytes. *Drug Metab Dispos* **36:**198-202.

Chu X, Bleasby K, and Evers R (2013) Species differences in drug transporters and implications for translating preclinical findings to humans. *Expert Opin Drug Metab Toxicol* **9:**237-252.

De Bruyn T, Ufuk A, Cantrill C, Kosa RE, Bi YA, Niosi M, Modi S, Rodrigues AD, Tremaine LM, Varma MVS, Galetin A, and Houston JB (2018) Predicting Human Clearance of Organic Anion Transporting Polypeptide Substrates Using Cynomolgus Monkey: In Vitro-In Vivo Scaling of Hepatic Uptake Clearance. *Drug Metab Dispos* **46:**989-1000.

Elsby R, Hilgendorf C, and Fenner K (2012) Understanding the critical disposition pathways of statins to assess drug-drug interaction risk during drug development: it's not just about OATP1B1. *Clin Pharmacol Ther* **92:**584-598.

Fallon JK, Smith PC, Xia CQ, and Kim MS (2016) Quantification of Four Efflux Drug Transporters in Liver and Kidney Across Species Using Targeted Quantitative Proteomics by Isotope Dilution NanoLC-MS/MS. *Pharm Res* **33:**2280-2288.

Grime K and Paine SW (2013) Species differences in biliary clearance and possible relevance of hepatic uptake and efflux transporters involvement. *Drug Metab Dispos* **41:**372-378.

Hagenbuch B and Meier PJ (2003) The superfamily of organic anion transporting polypeptides. *Biochim Biophys Acta* **1609:**1-18.

Hatanaka T (2000) Clinical pharmacokinetics of pravastatin: mechanisms of pharmacokinetic events. *Clin Pharmacokinet* **39:**397-412.

Hatorp V (2002) Clinical pharmacokinetics and pharmacodynamics of repaglinide. *Clin Pharmacokinet* **41:**471-483.

Higgins JW, Bao JQ, Ke AB, Manro JR, Fallon JK, Smith PC, and Zamek-Gliszczynski MJ (2014) Utility of Oatp1a/1b-Knockout and OATP1B1/3-Humanized Mice in the Study of OATP-Mediated Pharmacokinetics and Tissue Distribution: Case Studies with Pravastatin, Atorvastatin, Simvastatin, and Carboxydichlorofluorescein. *Drug Metabolism and Disposition* **42:**182-192.

Hirano M, Maeda K, Shitara Y, and Sugiyama Y (2006) Drug-drug interaction between pitavastatin and various drugs via OATP1B1. *Drug Metab Dispos* **34:**1229-1236.

Ieiri I, Higuchi S, and Sugiyama Y (2009) Genetic polymorphisms of uptake (OATP1B1, 1B3) and efflux (MRP2, BCRP) transporters: implications for inter-individual differences in the pharmacokinetics and pharmacodynamics of statins and other clinically relevant drugs. *Expert Opin Drug Metab Toxicol* **5:**703-729.

Iusuf D, van Esch A, Hobbs M, Taylor M, Kenworthy KE, van de Steeg E, Wagenaar E, and Schinkel AH (2013) Murine Oatp1a/1b uptake transporters control rosuvastatin systemic exposure without affecting its apparent liver exposure. *Mol Pharmacol* **83:**919-929.

Kalliokoski A, Neuvonen M, Neuvonen PJ, and Niemi M (2008) The effect of SLCO1B1 polymorphism on repaglinide pharmacokinetics persists over a wide dose range. *Br J Clin Pharmacol* **66:**818-825.

Kalliokoski A and Niemi M (2009) Impact of OATP transporters on pharmacokinetics. *Br J Pharmacol* **158:**693-705.

Kaneko K, Tanaka M, Ishii A, Katayama Y, Nakaoka T, Irie S, Kawahata H, Yamanaga T, Wada Y, Miyake T, Toshimoto K, Maeda K, Cui Y, Enomoto M, Kawamura E, Kawada N, Kawabe J, Shiomi S, Kusuhara H, Sugiyama Y, and Watanabe Y (2018) A Clinical Quantitative Evaluation of Hepatobiliary Transport of [(11)C]Dehydropravastatin in Humans Using Positron Emission Tomography. *Drug Metab Dispos* **46:**719-728.

Katoh M, Sawada T, Soeno Y, Nakajima M, Tateno C, Yoshizato K, and Yokoi T (2007) In vivo drug metabolism model for human cytochrome P450 enzyme using chimeric mice with humanized liver. *J Pharm Sci* **96:**428-437.

Kitamura S, Maeda K, Wang Y, and Sugiyama Y (2008) Involvement of multiple transporters in the hepatobiliary transport of rosuvastatin. *Drug Metab Dispos* **36:**2014-2023.

Kunze A, Huwyler J, Camenisch G, and Poller B (2014) Prediction of organic anion-transporting polypeptide 1B1- and 1B3-mediated hepatic uptake of statins based on transporter protein expression and activity data. *Drug Metab Dispos* **42:**1514-1521.

Li N, Zhang Y, Hua F, and Lai Y (2009) Absolute difference of hepatobiliary transporter multidrug resistance-associated protein (MRP2/Mrp2) in liver tissues and isolated hepatocytes from rat, dog, monkey, and human. *Drug Metab Dispos* **37:**66-73.

Luo Z, Zhang Y, Gu J, Feng P, and Wang Y (2015) Pharmacokinetic Properties of Single- and Multiple-Dose Pitavastatin Calcium Tablets in Healthy Chinese Volunteers. *Curr Ther Res Clin Exp* **77:**52-57.

Luvai A, Mbagaya W, Hall AS, and Barth JH (2012) Rosuvastatin: a review of the pharmacology and clinical effectiveness in cardiovascular disease. *Clin Med Insights Cardiol* **6:**17-33.

Martin PD, Warwick MJ, Dane AL, Hill SJ, Giles PB, Phillips PJ, and Lenz E (2003) Metabolism, excretion, and pharmacokinetics of rosuvastatin in healthy adult male volunteers. *Clin Ther* **25:**2822-2835.

Meier-Abt F, Mokrab Y, and Mizuguchi K (2005) Organic anion transporting polypeptides of the OATP/SLCO superfamily: identification of new members in nonmammalian species, comparative modeling and a potential transport mode. *J Membr Biol* **208:**213-227.

Ménochet K, Kenworthy KE, Houston JB, and Galetin A (2012a) Simultaneous Assessment of Uptake and Metabolism in Rat Hepatocytes: A Comprehensive Mechanistic Model. *Journal of Pharmacology and Experimental Therapeutics* **341:**2-15.

Ménochet K, Kenworthy KE, Houston JB, and Galetin A (2012b) Use of Mechanistic Modeling to Assess Interindividual Variability and Interspecies Differences in Active Uptake in Human and Rat Hepatocytes. *Drug Metabolism and Disposition* **40:**1744-1756.

Miyamoto M, Iwasaki S, Chisaki I, Nakagawa S, Amano N, and Hirabayashi H (2017) Comparison of predictability for human pharmacokinetics parameters among monkeys, rats, and chimeric mice with humanised liver. *Xenobiotica* **47:**1052-1063.

Morse BL, Cai H, MacGuire JG, Fox M, Zhang L, Zhang Y, Gu X, Shen H, Dierks EA, Su H, Luk CE, Marathe P, Shu YZ, Humphreys WG, and Lai Y (2015) Rosuvastatin Liver Partitioning in Cynomolgus Monkeys: Measurement In Vivo and Prediction Using In Vitro Monkey Hepatocyte Uptake. *Drug Metab Dispos* **43:**1788-1794.

Naritomi Y, Sanoh S, and Ohta S (2019) Utility of Chimeric Mice with Humanized Liver for Predicting Human Pharmacokinetics in Drug Discovery: Comparison with in Vitro-in Vivo Extrapolation and Allometric Scaling. *Biol Pharm Bull* **42:**327-336.

Neuvonen PJ, Niemi M, and Backman JT (2006) Drug interactions with lipid-lowering drugs: mechanisms and clinical relevance. *Clin Pharmacol Ther* **80:**565-581.

Niemi M, Pasanen MK, and Neuvonen PJ (2011) Organic anion transporting polypeptide 1B1: a genetically polymorphic transporter of major importance for hepatic drug uptake. *Pharmacol Rev* **63:**157-181.

Nishimura M, Yoshitsugu H, Yokoi T, Tateno C, Kataoka M, Horie T, Yoshizato K, and Naito S (2005) Evaluation of mRNA expression of human drug-metabolizing enzymes and transporters in chimeric mouse with humanized liver. *Xenobiotica* **35:**877-890.

Ohtsuki S, Kawakami H, Inoue T, Nakamura K, Tateno C, Katsukura Y, Obuchi W, Uchida Y, Kamiie J, Horie T, and Terasaki T (2014) Validation of uPA/SCID mouse with humanized liver as a human liver model: protein quantification of transporters, cytochromes P450, and UDP-glucuronosyltransferases by LC-MS/MS. *Drug Metab Dispos* **42:**1039-1043.

Okumura H, Katoh M, Sawada T, Nakajima M, Soeno Y, Yabuuchi H, Ikeda T, Tateno C, Yoshizato K, and Yokoi T (2007) Humanization of excretory pathway in chimeric mice with humanized liver. *Toxicol Sci* **97:**533-538.

Patilea-Vrana G and Unadkat JD (2016) Transport vs. Metabolism: What Determines the Pharmacokinetics and Pharmacodynamics of Drugs? Insights From the Extended Clearance Model. *Clin Pharmacol Ther* **100:**413-418.

Prueksaritanont T, Chu X, Evers R, Klopfer SO, Caro L, Kothare PA, Dempsey C, Rasmussen S, Houle R, Chan G, Cai X, Valesky R, Fraser IP, and Stoch SA (2014) Pitavastatin is a more sensitive and selective organic anion-transporting polypeptide 1B clinical probe than rosuvastatin. *British Journal of Clinical Pharmacology* **78:**587-598.

Riccardi K, Lin J, Li Z, Niosi M, Ryu S, Hua W, Atkinson K, Kosa RE, Litchfield J, and Di L (2017) Novel Method to Predict In Vivo Liver-to-Plasma K(puu) for OATP Substrates Using Suspension Hepatocytes. *Drug Metab Dispos* **45:**576-580.

Riede J, Camenisch G, Huwyler J, and Poller B (2017) Current In Vitro Methods to Determine Hepatic Kpuu: A Comparison of Their Usefulness and Limitations. *Journal of Pharmaceutical Sciences* **106:**2805-2814.

Salphati L, Chu X, Chen L, Prasad B, Dallas S, Evers R, Mamaril-Fishman D, Geier EG, Kehler J, Kunta J, Mezler M, Laplanche L, Pang J, Rode A, Soars MG, Unadkat JD, van Waterschoot RAB, Yabut J, Schinkel AH, and Scheer N (2014) Evaluation of Organic Anion Transporting Polypeptide 1B1 and 1B3 Humanized Mice as a Translational Model to Study the Pharmacokinetics of Statins. *Drug Metabolism and Disposition* **42:**1301-1313.

Samuelsson K, Pickup K, Sarda S, Swales JG, Morikawa Y, Schulz-Utermoehl T, Hutchison M, and Wilson ID (2012) Pharmacokinetics and metabolism of midazolam in chimeric mice with humanised livers. *Xenobiotica* **42:**1128-1137.

Sanoh S, Horiguchi A, Sugihara K, Kotake Y, Tayama Y, Ohshita H, Tateno C, Horie T, Kitamura S, and Ohta S (2012) Prediction of in vivo hepatic clearance and half-life of drug candidates in human using chimeric mice with humanized liver. *Drug Metab Dispos* **40:**322-328.

Shitara Y, Maeda K, Ikejiri K, Yoshida K, Horie T, and Sugiyama Y (2013) Clinical significance of organic anion transporting polypeptides (OATPs) in drug disposition: their roles in hepatic clearance and intestinal absorption. *Biopharm Drug Dispos* **34:**45-78.

Shitara Y and Sugiyama Y (2006) Pharmacokinetic and pharmacodynamic alterations of 3-hydroxy-3-methylglutaryl coenzyme A (HMG-CoA) reductase inhibitors: drug-drug interactions and interindividual differences in transporter and metabolic enzyme functions. *Pharmacol Ther* **112:**71-105.

Siddiqui N, Husain A, Chaudhry L, Alam MS, Mitra M, and Bhasin PS (2011) Pharmacological and Pharmaceutical Profile of Valsartan: A Review. *Journal of Applied Pharmaceutical Science* **1:**12-19.

Tateno C, Kawase Y, Tobita Y, Hamamura S, Ohshita H, Yokomichi H, Sanada H, Kakuni M, Shiota A, Kojima Y, Ishida Y, Shitara H, Wada NA, Tateishi H, Sudoh M, Nagatsuka S, Jishage K, and Kohara M (2015) Generation of Novel Chimeric Mice with Humanized Livers by Using Hemizygous cDNA-uPA/SCID Mice. *PLoS One* **10:**e0142145.

Tateno C, Yoshizane Y, Saito N, Kataoka M, Utoh R, Yamasaki C, Tachibana A, Soeno Y, Asahina K, Hino H, Asahara T, Yokoi T, Furukawa T, and Yoshizato K (2004) Near completely humanized liver in mice shows human-type metabolic responses to drugs. *Am J Pathol* **165:**901-912.

Uchida M, Tajima Y, Kakuni M, Kageyama Y, Okada T, Sakurada E, Tateno C, and Hayashi R (2018) Organic Anion–Transporting Polypeptide (OATP)–Mediated Drug-Drug Interaction Study between Rosuvastatin and Cyclosporine A in Chimeric Mice with Humanized Liver. *Drug Metabolism and Disposition* **46:**11-19.

van de Steeg E, van Esch A, Wagenaar E, Kenworthy KE, and Schinkel AH (2013) Influence of human OATP1B1, OATP1B3, and OATP1A2 on the pharmacokinetics of methotrexate and paclitaxel in humanized transgenic mice. *Clin Cancer Res* **19:**821-832.

Vildhede A, Wiśniewski JR, Norén A, Karlgren M, and Artursson P (2015) Comparative Proteomic Analysis of Human Liver Tissue and Isolated Hepatocytes with a Focus on Proteins Determining Drug Exposure. *J Proteome Res* **14:**3305-3314.

Wang L, Prasad B, Salphati L, Chu X, Gupta A, Hop CE, Evers R, and Unadkat JD (2015) Interspecies variability in expression of hepatobiliary transporters across human, dog, monkey, and rat as determined by quantitative proteomics. *Drug Metab Dispos* **43:**367-374.

Watanabe T, Kusuhara H, and Sugiyama Y (2010) Application of physiologically based pharmacokinetic modeling and clearance concept to drugs showing transporter-mediated distribution and clearance in humans. *J Pharmacokinet Pharmacodyn* **37:**575-590.

Yabe Y, Galetin A, and Houston JB (2011) Kinetic characterization of rat hepatic uptake of 16 actively transported drugs. *Drug Metab Dispos* **39:**1808-1814.

Yoshida K, Maeda K, and Sugiyama Y (2012) Transporter-mediated drug--drug interactions involving OATP substrates: predictions based on in vitro inhibition studies. *Clin Pharmacol Ther* **91:**1053-1064.

Yoshikado T, Maeda K, Furihata S, Terashima H, Nakayama T, Ishigame K, Tsunemoto K, Kusuhara H, Furihata KI, and Sugiyama Y (2017) A Clinical Cassette Dosing Study for Evaluating the Contribution of Hepatic OATPs and CYP3A to Drug-Drug Interactions. *Pharm Res* **34:**1570-1583.

Zimmerman EI, Hu S, Roberts JL, Gibson AA, Orwick SJ, Li L, Sparreboom A, and Baker SD (2013) Contribution of OATP1B1 and OATP1B3 to the disposition of sorafenib and sorafenib-glucuronide. *Clin Cancer Res* **19:**1458-1466.

Footnotes:

The work was supported by Vertex Pharmaceutical Company Limited and Chimeric Mouse with Humanized Liver (CMHL) Consortium.

Yoshio Morikawa is an employee of PhoenixBio Co., Ltd., Hiroshima, Japan. He provided PXB mice but did not have any additional role in conducting the experiment, performing the data analysis, and preparing the manuscript.

All other authors (B.F., R.P., W.D., Z.Y., C.Z., G.W., and S.K.) declare no competing interest

DMD Fast Forward. Published on December 29, 2020 as DOI: 10.1124/dmd.120.000276
This article has not been copyedited and formatted. The final version may differ from this version.

Figure legends:

Figure 1: Histograms comparing uptake clearance in PXB and C57 mouse hepatocytes for five OATP substrates, including rosuvastatin, pitavastatin, pravastatin, valsartan and repaglinide. Total uptake clearance (A), active uptake clearance (B) and % active uptake (C) are presented. Hepatocyte uptake of OATP substrates was measured at a single concentration of 0.1 µM, with exceptions for pravastatin (5 µM) and valsartan (1 µM) at four time points, including 0.5, 1, 1.5, and 2 min. Total and passive clearance was determined from the initial rate of uptake at 37°C in the absence and presence of the OATP inhibitor, 1 mM rifamycin SV. Data are mean +/- SD. *P < 0.05, C57 mouse hepatocytes uptake versus PXB mouse hepatocytes uptake.

Figure 2: Rosuvastatin liver-to-plasma K_{puu} in PXB and SCID mouse. Rosuvastatin was dosed to SCID mice at 15 and 30 mg/kg and PXB mice at 1.5 and 3 mg/kg. Plasma and liver concentrations of rosuvastatin were measured at 1 hr after dose. The data for each point was from one mouse, and average K_{puu} values are presented with SD as error bars. **P < 0.01, rosuvastatin liver-to-plasma K_{puu} in PXB versus SCID mouse

Figure 3: Pravastatin liver-to-plasma K_{puu} in PXB and SCID mouse. Pravastatin was dosed to SCID mice at 1.8, 3, 10, 20 and 40 mg/kg and PXB mice at 0.6 and 3 mg/kg. Plasma and liver concentrations of pravastatin were measured at 0.5 hr after dose. The average K_{puu} for SCID mice was calculated from the doses of 10, 20 and 40 mg/kg, and the average K_{puu} for PXB mice was calculated from the dose of 0.6 mg/kg. Each point was from one mouse, and average K_{puu} values are presented with SD as error bars. *P < 0.05, pravastatin liver-to-plasma K_{puu} in PXB versus SCID mouse

DMD Fast Forward. Published on December 29, 2020 as DOI: 10.1124/dmd.120.000276
This article has not been copyedited and formatted. The final version may differ from this version.

Figure 4: Pitavastatin liver-to-plasma K_{puu} in PXB and SCID mouse. Pitavastatin was dosed to SCID mice at 0.2 and 0.5 mg/kg and PXB mice at 0.1 and 0.2 mg/kg. Plasma and liver concentrations of pitavastatin were measured at 0.25 hr after dose. The data for each point was from one mouse, and average K_{puu} values are presented with SD as error bars.

Figure 5: Valsartan liver-to-plasma K_{puu} in PXB and SCID mouse. Valsartan was dosed to SCID mice at 8 mg/kg and PXB mice at 5 and 8 mg/kg. Plasma and liver concentrations of valsartan were measured at 0.5 hr after dose. The data for each point was from one mouse, and average K_{puu} values are presented with SD as error bars. $*P < 0.05$, valsartan liver-to-plasma K_{puu} in PXB versus SCID mouse

Figure 6: Repaglinide liver-to-plasma K_{puu} in PXB and SCID mouse. Repaglinide was dosed to SCID mice at 1 and 1.5 mg/kg and PXB mice at 0.8 mg/kg. Plasma and liver concentrations of repaglinide were measured at 0.5 hr after dose. The data for each point was from one mouse, and average K_{puu} values are presented with SD as error bars.

DMD Fast Forward. Published on December 29, 2020 as DOI: 10.1124/dmd.120.000276
This article has not been copyedited and formatted. The final version may differ from this version.

Tables

TABLE 1: Pharmacokinetic parameters after a single oral dose of OATP substrates with whole blood samples taken out to 24h in PXB and SCID mice. Data are mean ± SD.

OATP Substrate	Vehicle	Dose (mg/kg)	Strain	AUC (ng·h/ml)[a]	C_{max} (ng/ml)
Rosuvastatin	PBS	1.5	SCID	5.34 ± 4.50	3.12 ± 2.06
			PXB	84.2 ± 23.1	31.1 ± 6.1
		5	SCID	95.0 ± 48.0	13.0 ± 4.1
			PXB	469 ± 222	177 ± 51
Pravastatin	PBS	2	SCID	35.6*	27.8*
			PXB	174 ± 169	72.8 ± 12.0
		10	SCID	166.5 ± 42.3	28.7 ± 0.8
			PXB	386 ± 15	276 ± 51
Pitavastatin	0.5% MC	0.3	SCID	1.9 ± 0.3	5.22 ± 0.72
			PXB	92.0 ± 22.1	43.3 ± 1.5
		1	SCID	6.70 ± 0.40	15.1 ± 2.5
			PXB	449 ± 82	191 ± 27
		3	SCID	26.7 ± 5.3	60.1 ± 3.5
			PXB	1540 ± 147	742 ± 259
Valsartan	0.5%MC/0.02%SLS	10	SCID	364 ± 206	141 ± 82
			PXB	10742 ± 8487	5337 ± 1095
		50	SCID	1705 ± 902	285 ± 132
			PXB	44041 ± 11973	24367 ± 13880
Repaglinide	10% Ethanol/ 30% PEG400/ 20% Dextrose	0.5	SCID	18.6 ± 11.2	15.7 ± 1.18
			PXB	33.4 ± 16.1	33.8 ± 11.2
		5	SCID	425 ± 140	200 ± 66
			PXB	322 ±62	268 ± 79

[a] Dose normalized AUC are extrapolated to infinity

*reported with *n=1*, 2 out 3 animal's concentrations measured below levels of quantification

TABLE 2. Dose selections for liver-to-plasma K_{puu} studies in PXB and SCID mice

	Rosuvastatin		Pravastatin		Pitavastatin		Valsartan		Repaglinide	
Clinical C_{max} (ng/ml)	44		25		38		3250		65	
Human plasma F_u%	17.1		51.8		0.9		0.3		1.0	
Unbound C_{max} (ng/mL)	7.5		13.0		0.3		9.8		0.7	
T_{max} (h)	1		0.5		0.25		0.5		0.5	
	PXB	SCID	PXB	SCID	PXB	SCID	PXB	SCID	PXB	SCID
Dose (mg/kg)	1.5 & 3	15 & 30	0.6 & 3	1.8, 3, 10, 20, & 40	0.1 & 0.2	0.2 & 0.5	8	8	0.8	1 & 1.5

TABLE 3. Plasma protein binding and liver binding of Rosuvastatin, Pravastatin, Pitavastatin, Valsartan, and Repaglinide in PXB and SCID mice from *ex-vivo* binding assay with tissues collected at T_{max} (h). Data are mean ± SD.

	Rosuvastatin		Pravastatin		Pitavastatin		Valsartan		Repaglinide	
	PXB	SCID	PXB	SCID	PXB	SCID	PXB	SCID	PXB	SCID
F_u plasma (%)	7.14 ± 0.50	12.2 ± 2.5	37.0*	71.0 ± 7.9	1.05 ± 0.27	2.67 ± 0.47	0.37 ± 0.13	4.03 ± 0.66	0.85± 0.19	1.67 ± 0.66
F_u liver (%)	19.1 ± 4.0	23.2 ±2.6	27.6 ± 8.2	39.8 ± 4.8	2.05 ± 0.52	2.74 ± 0.20	16.2 ± 8.5	21.8 ± 4.1	0.64 ± 0.12	0.62 ± 0.08

*pooled sample of plasma from 3 animals

TABLE 4. Unbound plasma and liver drug concentrations of rosuvastatin, pravastatin, pitavastatin, valsartan, and repaglinide in PXB and SCID mice in liver-to-plasma K_{puu} studies with tissues collected at T_{max} (h). Data are mean ± SD.

	Rosuvastatin		Pravastatin		Pitavastatin		Valsartan		Repaglinide	
	PXB	SCID	PXB	SCID	PXB	SCID	PXB	SCID	PXB	SCID
Unbound plasma (ng/ml)	7.20 ± 2.70	17.1 ± 12.5	38.1 ± 13.8	23.6 ± 17.3	0.25 ± 0.12	0.47 ± 0.20	9.64 ± 5.92	4.74 ± 1.88	0.58 ± 0.12	1.73 ± 0.90
Unbound liver (ng/g)	167 ± 56	4572 ± 3417	169 ± 89	2871 ± 1239	4.02 ± 2.71	8.37 ± 3.04	791 ± 460	198 ± 136	1.58 ± 0.46	2.46 ± 1.16

Table 5. Comparison of liver-to-plasma K_{puu} of OATP substrates in PXB, SCID mouse and human.

OATP Substrate	Liver-to-Plasma K_{puu} in PXB Mouse	Liver-to-Plasma K_{puu} in SCID Mouse	Liver-to-Plasma K_{puu} in Human
Rosuvastatin	23	268	43 (PET), 10 (PK/PD)
Pravastatin	4.4	121	5.3 (PK/PD), 7 (DHP, PET)
Pitavastatin	16	18	2.10-14.58, 1.7 (In vitro hepatocytes)
Valsartan	82	42	80 (In vitro hepatocytes)
Repaglinide	2.7	1.4	1.1 (In vitro hepatocytes)

DMD Fast Forward. Published on December 29, 2020 as DOI: 10.1124/dmd.120.000276
This article has not been copyedited and formatted. The final version may differ from this version.

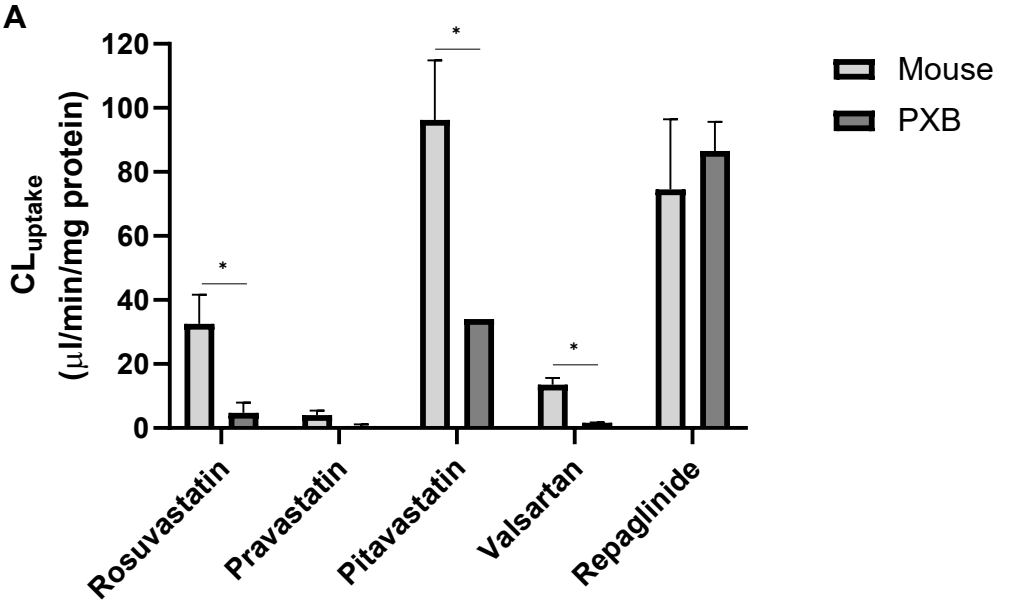
A
120
100
80
60
40
20
0
CLuptake
(μl/min/mg protein)
*
*
*
Mouse
PXB
Rosuvastatin
Pravastatin
Pitavastatin
Valsartan
Repaglinide

Figure 1A

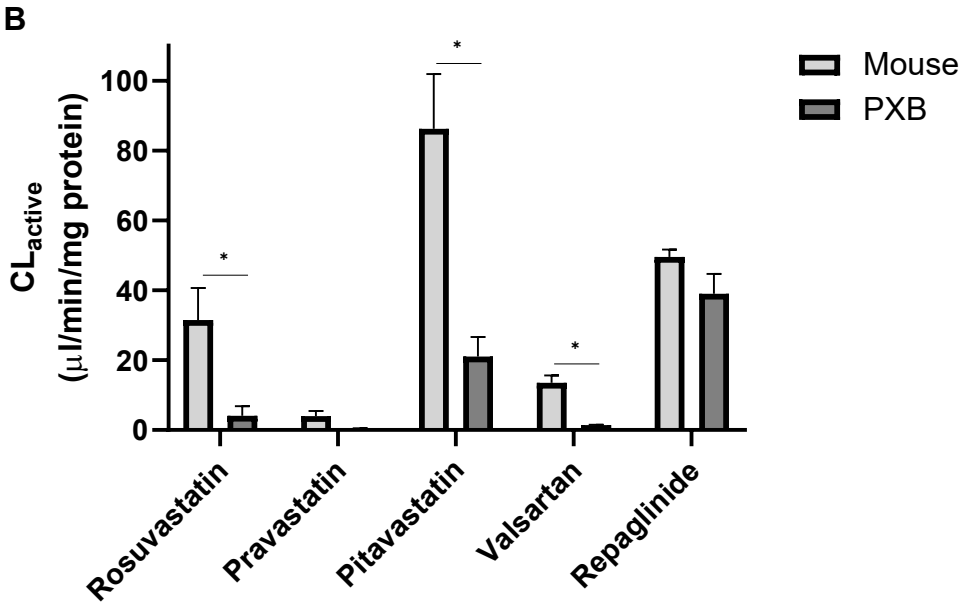
B
Mouse
PXB
CL_{active} (μl/min/mg protein)
100
80
60
40
20
0
*
*
*
Rosuvastatin
Pravastatin
Pitavastatin
Valsartan
Repaglinide

Figure 1B

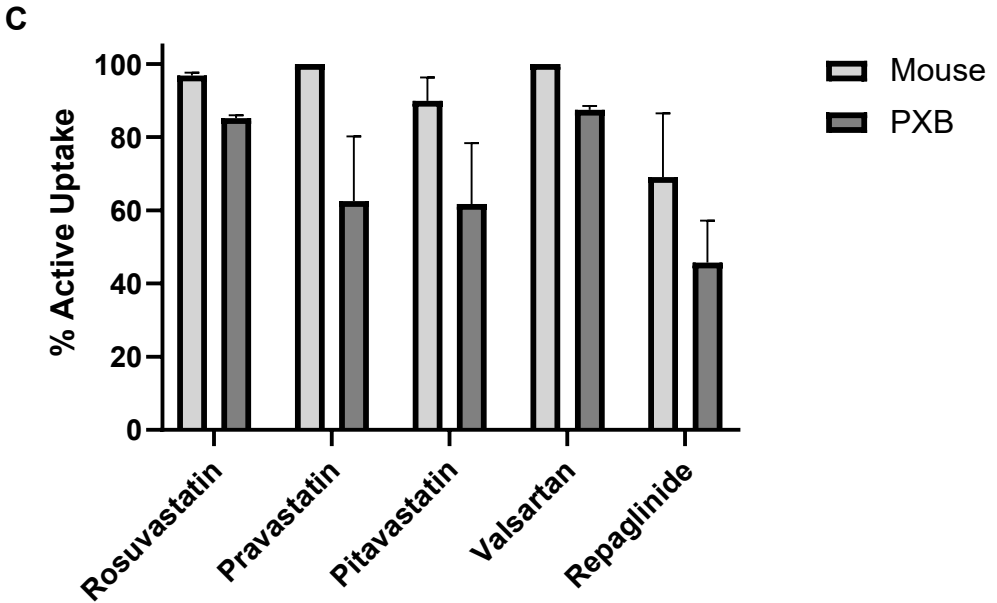
C
% Active Uptake
100
80
60
40
20
0
Mouse
PXB
Rosuvastatin
Pravastatin
Pitavastatin
Valsartan
Repaglinide

Figure 1C

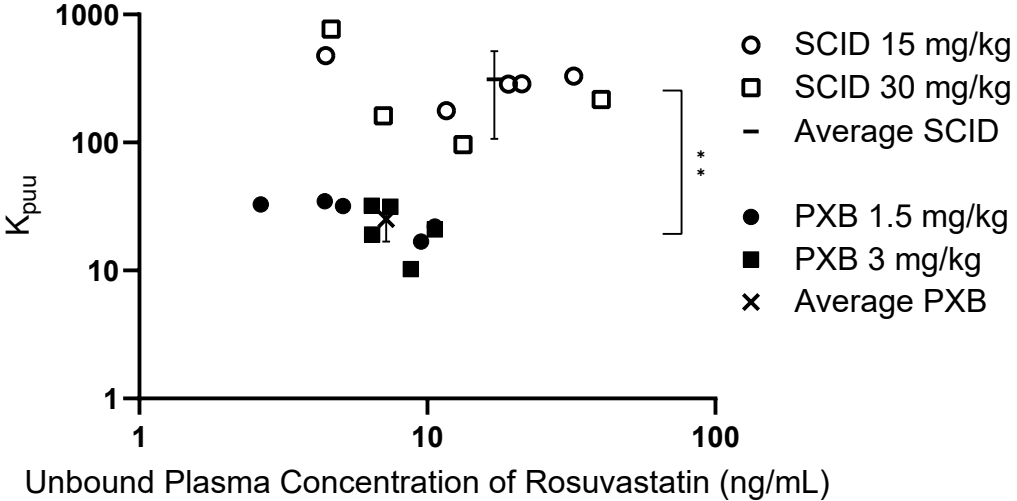
1000
100
10
1
K_{puu}
1
10
100
Unbound Plasma Concentration of Rosuvastatin (ng/mL)
**
SCID 15 mg/kg
SCID 30 mg/kg
Average SCID
PXB 1.5 mg/kg
PXB 3 mg/kg
Average PXB

Figure 2

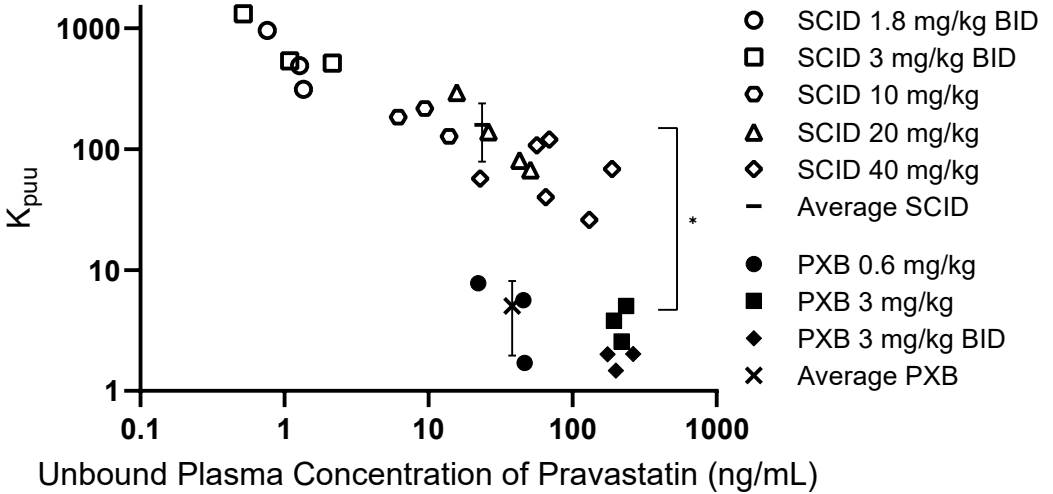
1000
100
10
1
K_{puu}
0.1
1
10
100
1000
Unbound Plasma Concentration of Pravastatin (ng/mL)
*
SCID 1.8 mg/kg BID
SCID 3 mg/kg BID
SCID 10 mg/kg
SCID 20 mg/kg
SCID 40 mg/kg
Average SCID
PXB 0.6 mg/kg
PXB 3 mg/kg
PXB 3 mg/kg BID
Average PXB

Figure 3

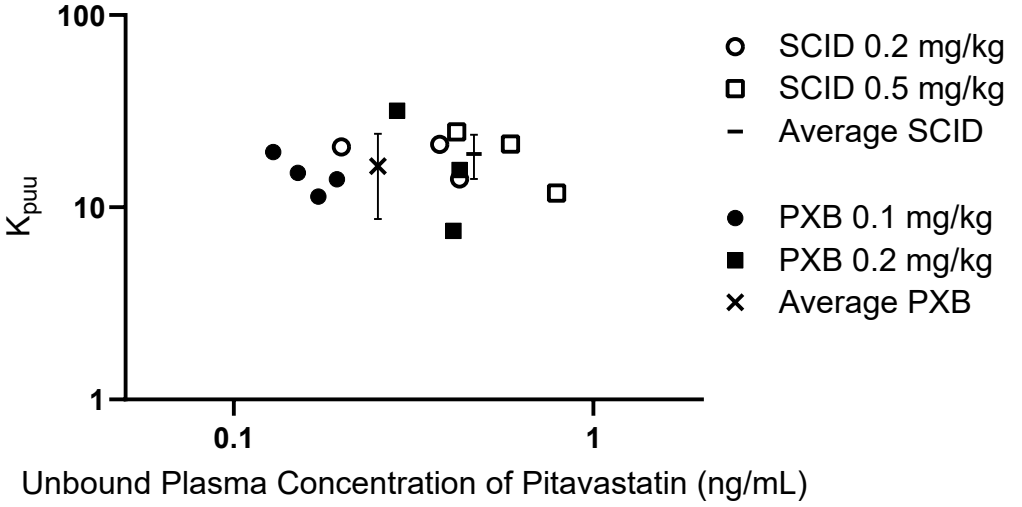
100
10
1
0.1
1
K_{puu}
Unbound Plasma Concentration of Pitavastatin (ng/mL)
SCID 0.2 mg/kg
SCID 0.5 mg/kg
Average SCID
PXB 0.1 mg/kg
PXB 0.2 mg/kg
Average PXB

Figure 4

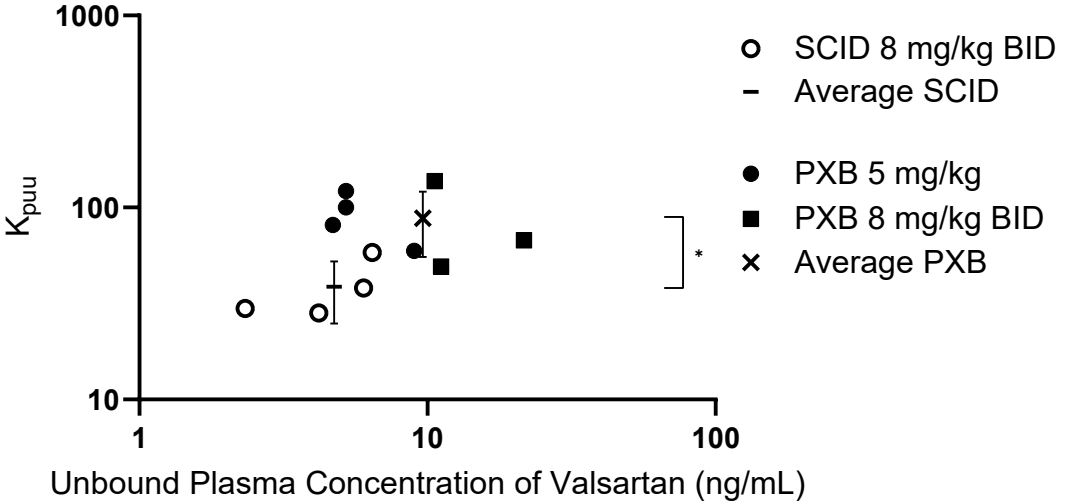
1000
100
10
K_{puu}
1
10
100
Unbound Plasma Concentration of Valsartan (ng/mL)
SCID 8 mg/kg BID
Average SCID
PXB 5 mg/kg
PXB 8 mg/kg BID
Average PXB
*

Figure 5

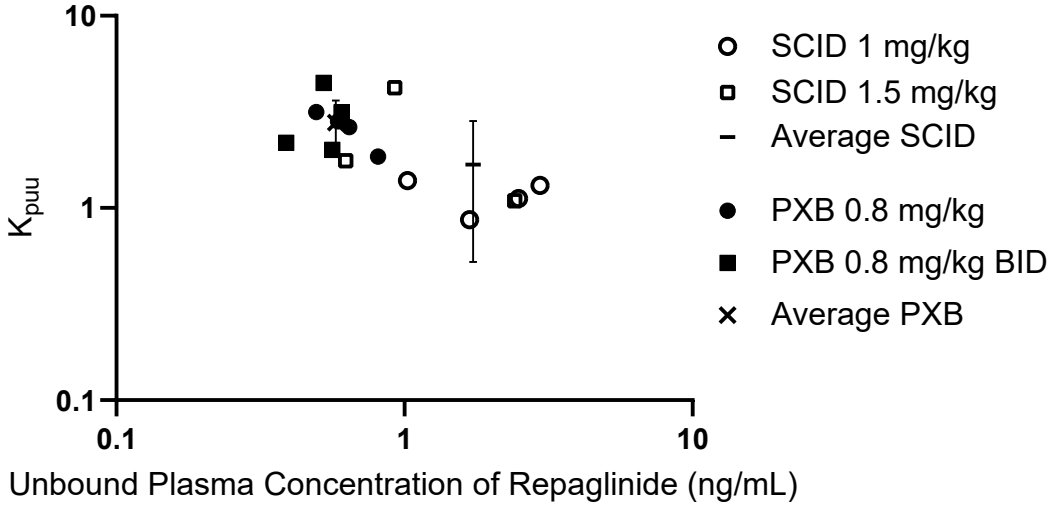
10
1
0.1
K_{puu}
0.1
1
10
Unbound Plasma Concentration of Repaglinide (ng/mL)
SCID 1 mg/kg
SCID 1.5 mg/kg
Average SCID
PXB 0.8 mg/kg
PXB 0.8 mg/kg BID
Average PXB

Figure 6